

In silico investigation on the effect of p27 phosphorylation in regulating Cdk2/CyclinA complex

Khyati Goswami, Prerana Kalita, Trishna Deka & Venkata Satish Kumar Mattaparthi*

Molecular Modelling and Simulation Laboratory, Department of Molecular Biology and Biotechnology,
Tezpur University, Tezpur-784 028, Assam, India

Received 02 April 2025; revised 03 July 2025

p27 is an intrinsically disordered protein which belongs to the Cip/Kip family. It inhibits the cyclin-dependent kinase (Cdk)/cyclin complexes which results in the regulation of cell cycle, during the G1 to S phase transition. Phosphorylation of p27 at specific sites such as Y74, Y88, T187, and P188 may alter its function. *In vitro* studies showed that phosphorylation of p27 at residues Y74 and Y88 resulted in enhancement of Cdk2 activity. However, the exact molecular details are unknown. This study uses molecular dynamics (MD) simulation and trajectory analyses to study the effect of phosphorylation of p27 at the Y74 and Y88 residues. We carried out MD simulation for 50 ns using AMBER20, and performed root mean square deviation (RMSD), root mean square fluctuation (RMSF), radius of gyration (Rg), solvent-accessible surface area (SASA), and hydrogen bonding analyses. We studied protein-protein interaction using PDBsum server. It has been found that there is an increase in binding affinity of phosphorylated p27 for Cdk2, but it weakens the Cdk2/cyclin A association. We observed shifts in RMSD, RMSF, and hydrogen bonding patterns which shows that there are conformational changes, thus providing insights into the increase in Cdk2 activity and its regulatory role in cell cycle.

Keywords: Cell cycle, Cyclin-dependent kinase inhibitors, Intrinsically disordered proteins, Tyrosine, Molecular dynamics simulation

Cdk/cyclin complexes are essential for regulating the eukaryotic cell cycle^{1,2}. In eukaryotes, cell cycle progression depends on the activity of cyclin-dependent kinases (Cdk), a family of serine/threonine kinases that convey signals to biochemically regulate advancement via the gap phases by phosphorylating certain substrate groups^{1,3}. Cyclins, which are expressed differently in oscillatory waves during several stages of the cell cycle, bind to the Cdks to activate them¹. Inhibitors referred to as Cdk/cyclin Complex Inhibitors (CKIs) exist in addition to the activating Cdks⁴. The INK4 family and the Cip/Kip family are the two major families into which these inhibitors fall¹. Proteins like p18 belong to the INK4 family, which has a structure made up of folded ankyrin repeats that bind to Cdk4 and Cdk6 specifically to inhibit their activity¹. However, proteins like p21, p27, and p57, which are members of the Cip/Kip family, are intrinsically disordered^{1,5}. Their ability to interact with different Cdk/cyclin

complexes and produce inhibitory effects is a result of their lack of a stable structure¹. It is interesting to note that p21 and p27 are involved in the correct assembly and localization of Cdk4 and 6/cyclinD complexes in addition to inhibiting them^{1,6,7}. Phosphorylated p27 (pY-p27), Cdk4, and cyclinD1 ternary complexes are enzymatically active because phosphorylation of Y74 and Y88 destabilizes the Cdk-binding domain of p27^{1,6,7}. In contrast to the widely accepted theory that proteins fold into a single native shape in order to carry out their functions, intrinsically disordered proteins (IDPs) are a class of proteins that do not have a fixed three-dimensional (3-D) structure under physiological settings^{8,9}. Without partner binding, intrinsically disordered protein regions (IDRs) cannot fold spontaneously into globular 3-D structures^{10,11}. Moreover, it has been discovered that IDPs are involved in a wide range of biological functions, including signalling, cell cycle control, recognition, and regulation¹²⁻¹⁴. IDPs and their Intrinsically Disordered Regions (IDRs) often contain conserved sequences known as short linear motifs (SLiMs)¹⁵. The motifs which are consecutively comprised of 3-10 amino acid residues and are important as they may be able to bind to other molecules¹. Many

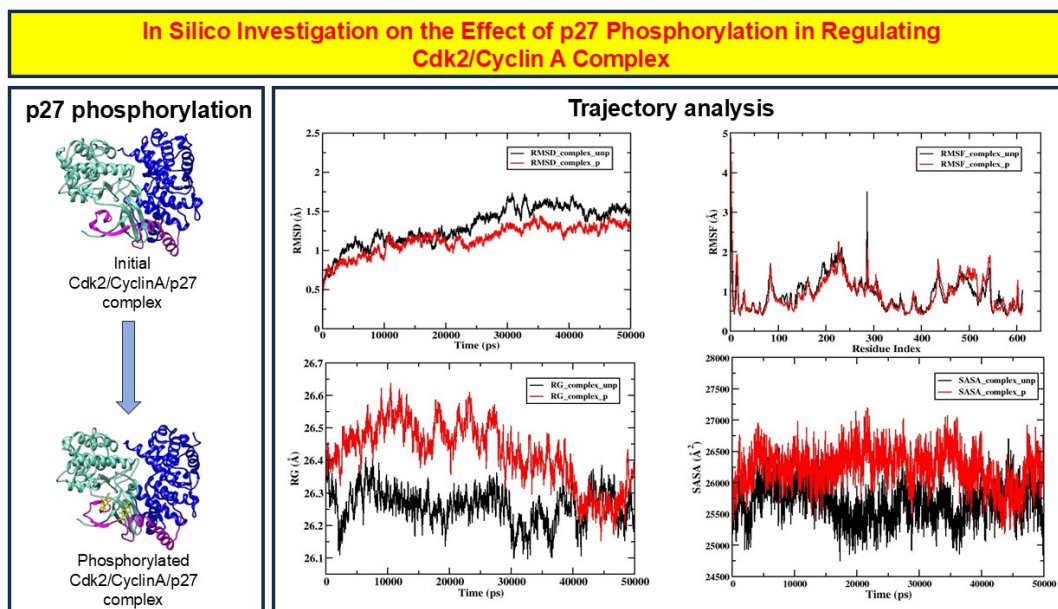
*Correspondence:

Phone: -91-3712-275443 (O), +91-8811806866 (M)

Fax: -91-3712-267005/267006

E-mail: mvenkatasatishkumar@gmail.com, venkata@tezu.ernet.in

Suppl. data available on respective page of NOPR



Graphical abstract

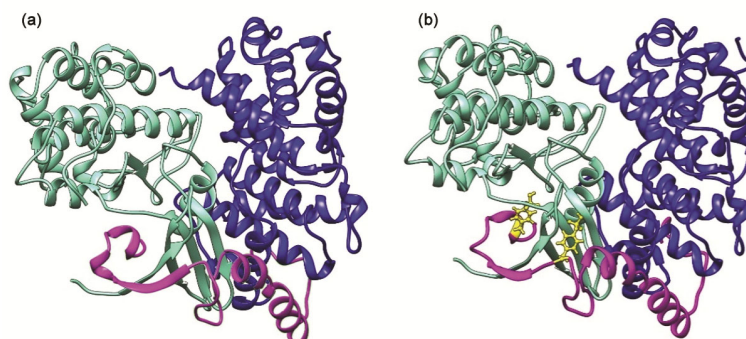


Fig. 1 — Three-dimensional structure of (a) initial Cdk2/cyclinA/p27 complex: Aquamarine Cdk2 (Chain A), Blue cyclin A (Chain B), and Magenta p27 (Chain C); and (b) phosphorylated Cdk2/cyclinA/p27 complex: Aquamarine Cdk2 (Chain A), Blue cyclin A (Chain B), and Magenta p27 (Chain C) and Yellow phosphorylated Tyrosine residues

functions in the cells such as cell signalling, protein targeting, degradation and cleavages are facilitated by the SLiMs^{1,15}. For the regulation of cell cycle, the interaction between Cdks, cyclins and their inhibitors are crucial¹. The intrinsically disordered proteins also contribute to the functioning of this system¹. The role of phosphorylation of p27 in the regulation of Cdk2/cyclin A complex can be studied by conducting Molecular Dynamics simulations. The current study employs AMBER force field ff99SB¹⁶, TIP3P¹⁷ and phosaa10^{18,19} parameters for performing MD simulations. This study is an *in silico* investigation of the role of phosphorylated and unphosphorylated p27 in the modulation of Cdk2/cyclinA complex. The activation of Cdk2 by cyclinA is essential for transition of cells into the S phase and in the synthesis of DNA²⁰. p27 blocks the activity of Cdk2 by

changing the kinase's N lobe shape and blocking the active site by putting the side chain of tyrosine 88 (Y88) into the ATP binding pocket²⁰. Understanding how p27 functions in different phosphorylation states could provide insights into its regulatory mechanisms and how it influences cell cycle progression.

Materials and Methods

The three-dimensional crystal structure of the Cdk2/cyclin A/p27 complex, with a resolution of 2.30 Å, was obtained from the Research Collaboratory for Structural Bioinformatics Protein Data Bank (RCSB PDB; www.rcsb.org)²¹ under the accession ID 1JSU (Fig. 1A). This structure served as the initial model structure for constructing the phosphorylated variant of the complex used in this study. The retrieved

complex is composed of three polypeptide chains: chain A represents cyclin-dependent kinase 2 (Cdk2), chain B corresponds to cyclin A, and chain C represents the intrinsically disordered protein p27, a known inhibitor of Cdk/cyclin complexes.

Phosphorylation of p27 in IJSU

To simulate the phosphorylation-dependent structural changes in the complex, specific post-translational modifications were introduced into the original structure. In particular, tyrosine residues at positions 74 and 88 on the p27 subunit (chain C) were phosphorylated to reflect biologically relevant phosphorylation events previously reported to influence p27's interaction with the Cdk2/cyclinA complex. The phosphorylation was carried out using the *xleap* module from the AMBER20 software package²², which allows for precise parameterization, incorporation of non-standard residues such as phosphotyrosine, removal of steric hindrance and relaxation of the portion of the structure that was built. Following the introduction of phosphorylation, the modified structure was carefully examined and validated for structural integrity. The phosphorylated complex was visualized and subjected to preliminary analysis using the molecular modeling program UCSF Chimera²³, which provides interactive graphical exploration of molecular assemblies. The final phosphorylated model prepared for molecular dynamics simulation, is shown in (Fig. 1B).

Molecular dynamics simulations

Molecular dynamics (MD) simulations have emerged as a powerful computational approach in structural biology and computational biophysics. They enable the investigation of the dynamic behaviour of biomolecules, such as proteins, nucleic acids, lipids and their complexes, at atomic resolution over time, providing insights that are often inaccessible through experimental techniques alone. In this study, the two systems: the unphosphorylated and the phosphorylated forms of p27 bound to the Cdk2/cyclinA complex were subjected to MD simulation. The main objective of the work was to investigate how phosphorylation of p27 at tyrosine residues 74 and 88 influences the dynamic behaviour and interactions within the complex. An essential requirement for MD simulation is the selection of a suitable force field that can clearly represent the molecular environment and interactions. To precisely model the dynamics of the phosphorylated residues,

the *phosaa10*^{18,19} parameter set was combined with the AMBER ff99SB¹⁶ force field. We carried out system preparation using AMBER20's Leap module, where the protein was immersed in TIP3P¹⁷ water box, maintaining a minimum distance of 10 Å between the solute and the box edge to ensure proper hydration. Finally, to enable proper analysis of the protein's stability and interactions with the solvent, the system was neutralised by adding counter ions.

Energy minimization

System optimization was performed using a dual-stage minimisation strategy. The first stage involved 1,000 steps of steepest descent (SD), followed by 1,000 steps of the conjugate gradient (CG) method, maintaining a harmonic restraint of 2 kcal/mol/Å². This enabled the solvent molecules and counter ions to relax and resolve local steric clashes without changing the solute's conformation. In the second stage, unrestrained full-system minimization was performed, consisting of 500 steps of SD followed by 4,500 steps of CG, to eliminate steric clashes and unfavourable contacts.

Heating and equilibration

The minimized systems were gradually heated from 0 K to 300 K under constant volume conditions (NVT ensemble). Harmonic restraints (10 kcal/mol/Å²) were applied to solute atoms during heating to stabilize the protein structure. Following heating, the systems underwent equilibration under constant pressure and temperature (NPT ensemble) using three successive equilibration phases, each lasting 3,000 ps, with a reduced restraint force constant of 5 kcal/mol/Å². Subsequently, a short 1 ns pre-production equilibration was performed under unrestrained NPT conditions at 300 K and 1 atm to stabilize system density and volume.

Production run

The final production MD simulations were run for 50 nanoseconds under NPT conditions without any positional restraints. All covalent bonds involving hydrogen atoms were constrained using the SHAKE algorithm²⁴, allowing for a simulation time step of 2 femtoseconds (fs). Temperature and pressure were maintained using the Berendsen thermostat and barostat²⁵, with coupling constants of 0.5 ps for temperature control and 0.2 ps for pressure relaxation. Trajectory snapshots were recorded at 10 picoseconds interval throughout the simulation.

Analysis of MD simulation trajectories

The conformational dynamics and key structural features of both the unphosphorylated and phosphorylated complexes were analyzed using the 50 ns MD trajectory files. Post-simulation analyses were performed with the PTRAJ and CPPTRAJ²⁶ modules of the AMBER software suite. The evaluated parameters included Root Mean Square Deviation (RMSD), Root Mean Square Fluctuation (RMSF), inter- and intra-molecular hydrogen bonding, and Solvent Accessible Surface Area (SASA). All graphs and plots were generated using the xmgrace plotting software.

Results and Discussion

Conformational analysis of Cdk2/cyclin A/p27 (unphosphorylated) and Cdk2/cyclin A/p27 (phosphorylated)

The conformational integrity and flexibility of p27 are regulated by tyrosine phosphorylation. p27 phosphorylation at Tyr88 partially reactivates Cdk2 (~20%), while dual phosphorylation at both Tyr74 and Tyr88 increases this to 43%^{27,28}. These findings suggest that p27 does not function solely as a steady inhibitor of the Cdk2/cyclinA complex; instead, it operates as an effective regulator for Cdk2 activity. We analyzed the trajectory files obtained in the 50 ns molecular dynamics (MD) for both the unphosphorylated and phosphorylated states of the Cdk2/cyclin A/p27 complex. The conformational behaviour of the phosphorylated and unphosphorylated systems throughout the simulation period is illustrated in (Fig. 2A & 2B), respectively. All the preliminary analyses including root mean square deviation (RMSD), root mean square fluctuation (RMSF), radius of gyration (Rg), inter- and intra-molecular hydrogen bonding, and solvent accessible surface area (SASA) were evaluated to assess the nature of the simulation.

RMSD analysis

Taking the initial structures of Cdk2/cyclin A/p27 complexes, we calculated the root mean square deviation (RMSD) for all C α atoms both in the phosphorylated and unphosphorylated states. RMSD is an important parameter to predict the overall structural stability of the system over the simulation period, reflecting conformational deviations from the starting configuration. Figure 3 presented the RMSD profiles for both the complexes. During the course of 50 ns simulation, both complexes showed RMSD values converging around 1.5 Å, which shows a high degree of structural stability. The phosphorylated

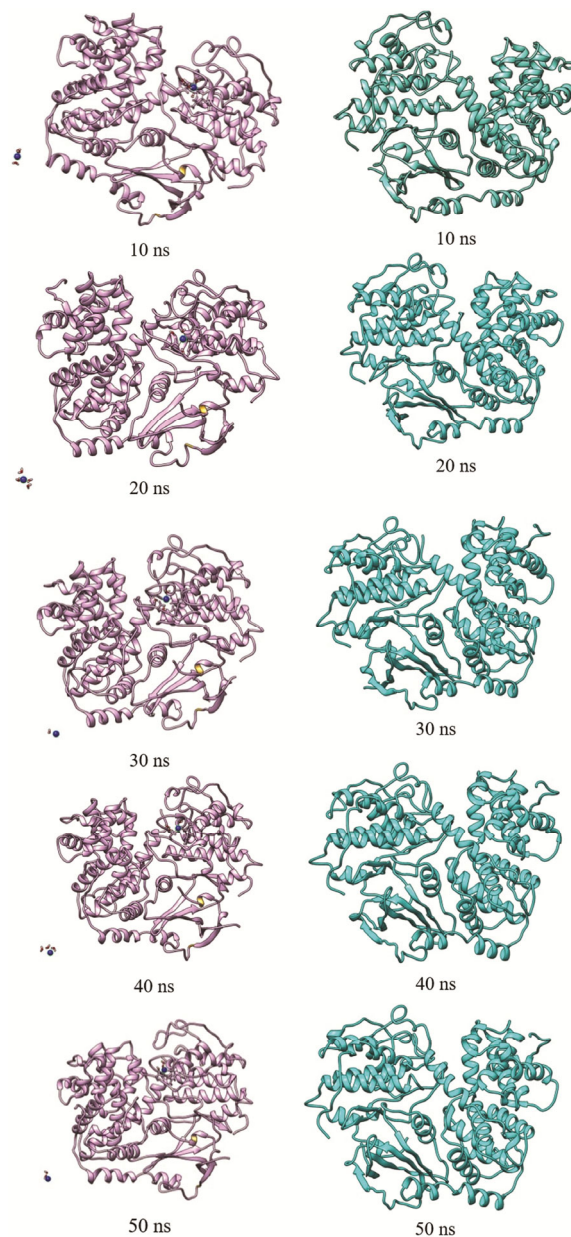


Fig. 2 — Conformational snapshots of Cdk2/cyclin A/p27 complex at discrete time interval of 10 ns during the course of 50 ns of MD simulation (a) Phosphorylated; and (b) Unphosphorylated

complex exhibited lower RMSD values compared to the unphosphorylated form, specifying that phosphorylation provides additional structural stability. This stabilization is a result of favourable conformational adjustments within the trimeric complex, which consists of Cdk2 (chain A), cyclin A (chain B), and p27 (chain C). The RMSD plots of individual chains in both phosphorylated and unphosphorylated states are presented in the (Suppl. Figs. S1 & S2), respectively.

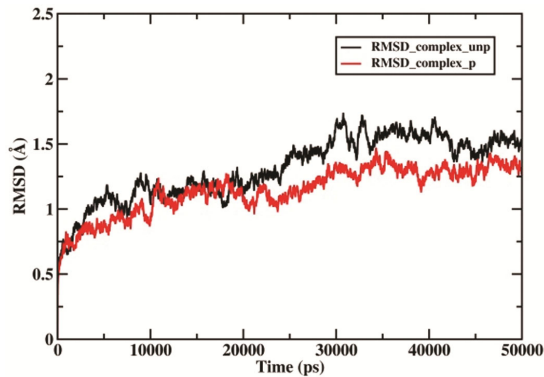


Fig. 3 — RMSD plots for the unphosphorylated (unp-black) and phosphorylated (p-red) complexes

RMSF analysis

The flexibility of individual residues within the protein complexes is evaluated by Root Mean Square Fluctuation (RMSF) analysis. RMSF calculates the average deviation of each atom from its mean position throughout the simulation. This offers insights into local mobility and dynamic behaviour at the residue level. The RMSF profiles for the unphosphorylated and phosphorylated complexes are presented in (Fig. 4A & 4B), respectively. RMSF values remained coherent across individual chains, while the p27 subunit (chain C) demonstrated a significant reduction in flexibility in its phosphorylated form. This confined decrease in RMSF suggests a

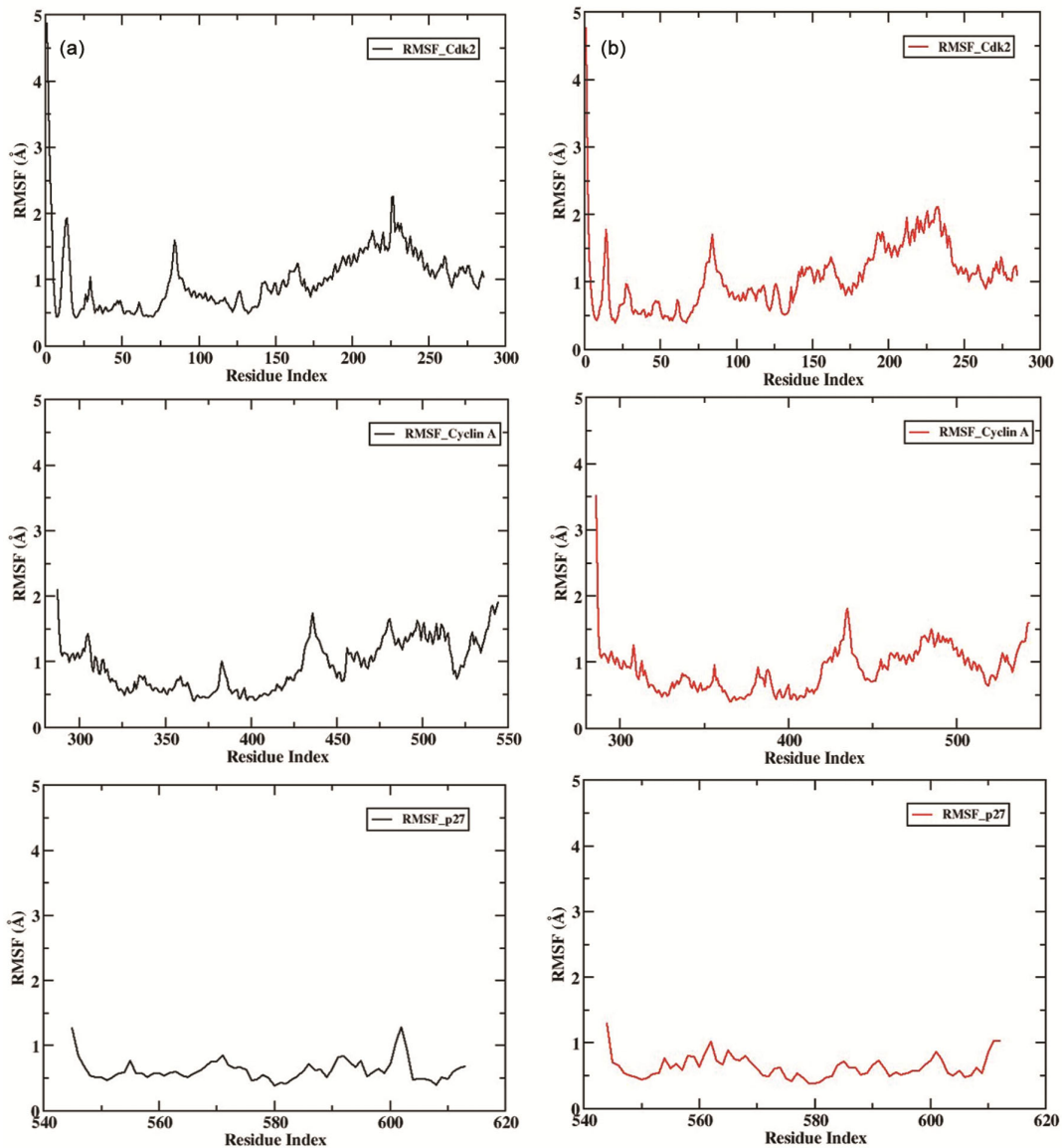


Fig. 4 — Backbone RMSF's for (a) Unphosphorylated (black) Cdk2 (chain A), cyclin A (chain B), and p27 (chain C); and (b) phosphorylated (red) Cdk2 (chain A), cyclin A (chain B), and p27 (chain C)

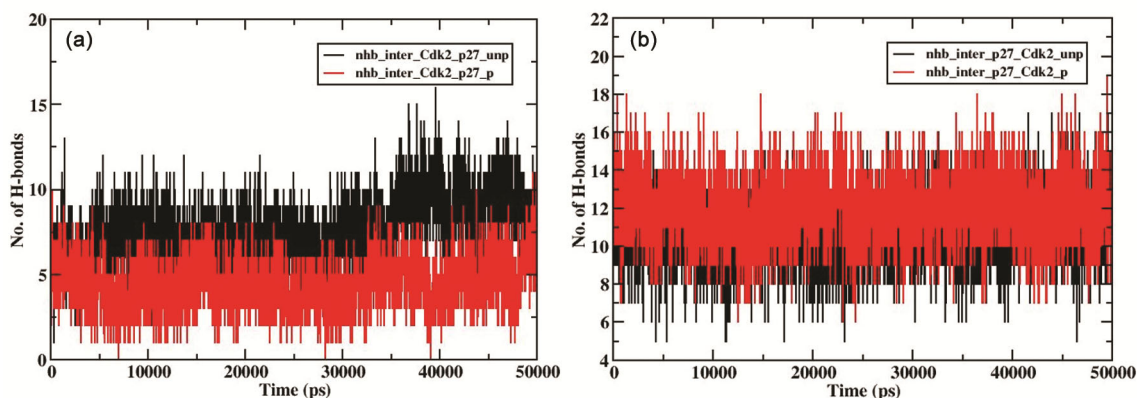


Fig. 5 — Number of intermolecular hydrogen bonds (a) between Cdk2 as donor and p27 as acceptor; and (b) between p27 as donor and Cdk2 as acceptor in both unphosphorylated (black) and phosphorylated (red) complexes

phosphorylation-dependent conformational tightening of the p27 inhibitor.

Hydrogen bond Analysis

We observed intra- and intermolecular hydrogen bonding patterns in the unphosphorylated and phosphorylated forms of the Cdk2/cyclin A/p27 complex. Special attention was given to intermolecular interactions between Cdk2 and p27 (chain C)²⁷ as the phosphorylated tyrosine residues in p27 are located near the ATP-binding pocket of Cdk2²⁷ (chain A). To find out the directional nature of these interactions, hydrogen bonding patterns were categorized into two donor-acceptor configurations. First, taking Cdk2 as the donor and p27 as the acceptor, and second, taking p27 as the donor and Cdk2 as the acceptor. As presented in Figure 5A and 5B, the p27 (donor)-Cdk2 (Acceptor) interface consistently maintained more interactions than the Cdk2 (donor)- p27 (acceptor) pairing. In addition to intermolecular hydrogen bonding, we also analyzed intramolecular hydrogen bonds within each individual chain to assess local structural integrity in both states. The results of this analysis are given in (Suppl. Figs. S3 & S4).

Radius of Gyration (Rg) analysis

The overall compactness of a protein is reflected by the radius of gyration which measures the average distance of its atoms from the center of mass²⁹. The Rg plots for both the unphosphorylated and phosphorylated Cdk2/cyclin A/p27 complexes are depicted in (Fig. 6). As apparent from the plot, the Rg values for both systems settle around 26.3 Å. This stability suggests that phosphorylation does not give rise to significant alterations in the global compactness of the complex. These findings also

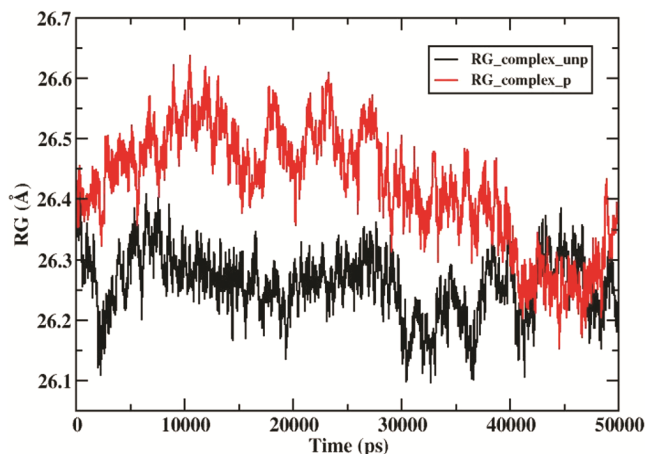


Fig. 6 —Rg plots for unphosphorylated (black) and phosphorylated (red) complexes

imply that the structural integrity and overall globular architecture of the complexes remain robust, largely unaffected by the phosphorylation state of p27.

SASA analysis

Solvent Accessible Surface Area (SASA) measures the surface area of a biomolecule that is accessible to solvent molecules, typically modeled as a spherical probe with a radius equivalent to that of a water molecule³⁰. It reveals exposure of residues to the solvent environment, which can reflect conformational changes or structural rearrangements. Figure 7 shows SASA in unphosphorylated and phosphorylated (Y74/Y88) Cdk2/cyclin A/p27 complexes. The results exhibit no significant difference in the overall SASA values between the two states, implying phosphorylation of p27 at Y74 and Y88 does not substantially perturb the complex's solvent exposure or tertiary structure.

Protein-protein interaction study

To investigate the relationship between Cdk2 (chain A) and p27 (chain C), both prior to and following phosphorylation, we conducted protein-protein interaction analyses using the PDBsum server³¹. The results are shown in (Fig. 8 and Table 1).

The Figure 8 and Table 1 present comparative interfacial interaction data between Cyclin-dependent kinase 2 (Cdk2) and the cyclin-dependent kinase inhibitor p27, in the unphosphorylated and phosphorylated complex systems. The modulation of the Cdk2-p27 interface through phosphorylation is central to its regulatory function in the cell cycle. Upon phosphorylation, the interface area increases, particularly within Cdk2, indicating a tighter and more stable complex. This stability is achieved by a higher density of salt bridges and the formation of six additional hydrogen bonds, which enhance the precision of molecular recognition. The rise in non-bonded contacts further contributes to a more compact and less flexible interface. These post-translational modifications stabilize the complex, providing a structural basis for enhanced inhibitory or regulatory effect of p27.

The interaction between Cdk2 and cyclin A in the phosphorylated and unphosphorylated complex

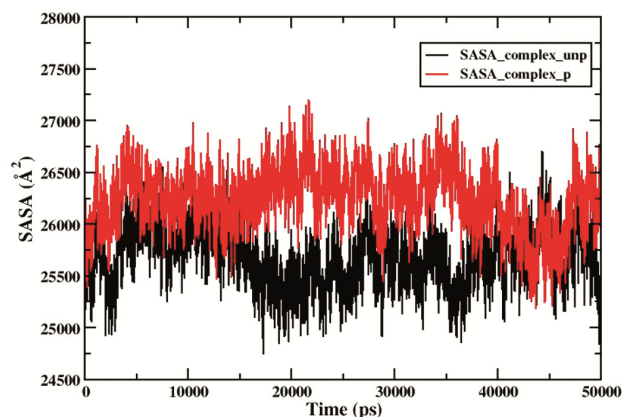


Fig. 7 —SASA plots for both unphosphorylated (black) and phosphorylated (red) complexes

systems were also analyzed. A comparative analysis of the molecular interactions at the interface between Cdk2 (Chain A) and Cyclin A (Chain B) are shown in (Table 2 and Fig. 9). These interactions are crucial for the structural stability and functional regulation of the

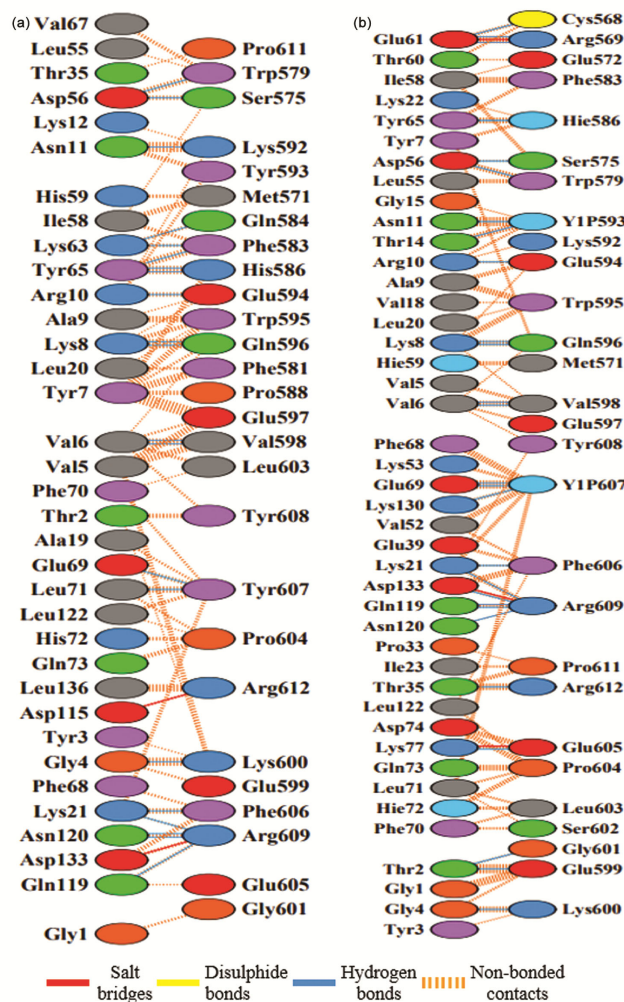


Fig. 8 — Interactive residues between chain A (Cdk2) and chain C(p27) (a) unphosphorylated system; and (b) phosphorylated system as predicted by PDBsum server. Molecular interactions such as hydrogen bonds, non-bonded contacts and salt bridges are considered here

Table 1 — Interface plot statistics for both unphosphorylated and phosphorylated Cdk2/cyclin A/p27 complexes. The plot shows the total number of interface residues, interface area, number of salt bridges, and total non-bonded contacts as predicted by PDBsum server

Complex	Chain	Interface statistics					
		No. of interface residues	Interface area (Å ²)	No. of salt bridges	No. of disulfide bonds	No. of hydrogen bonds	No. of non-bonded contacts
Unphosphorylated	Cdk2 (Chain A)	35	1658	2	-	21	240
	p27 (Chain C)	27	1720	-	-	-	-
Phosphorylated	Cdk2 (Chain A)	43	1902	3	-	27	255
	p27 (Chain C)	28	2067	-	-	-	-

Table 2 — Interface statistics for unphosphorylated and phosphorylated Cdk2/cyclin A/p27 complexes. The plot displays the total number of interface residues, interface area, number of salt bridges, and total non-bonded contacts as predicted by PDBsum server

Complex	Chain	Interface statistics					
		No. of interface residues	Interface area (Å ²)	No. of salt bridges	No. of disulfide bonds	No. of hydrogen bonds	No. of non-bonded contacts
Unphosphorylated	Cdk2 (Chain A)	33	1721	4	-	18	198
	Cyclin A (Chain B)	32	1734	-	-	-	
Phosphorylated	Cdk2 (Chain A)	32	1644	4	-	17	165
	Cyclin A (Chain B)	26	1654	-	-	-	

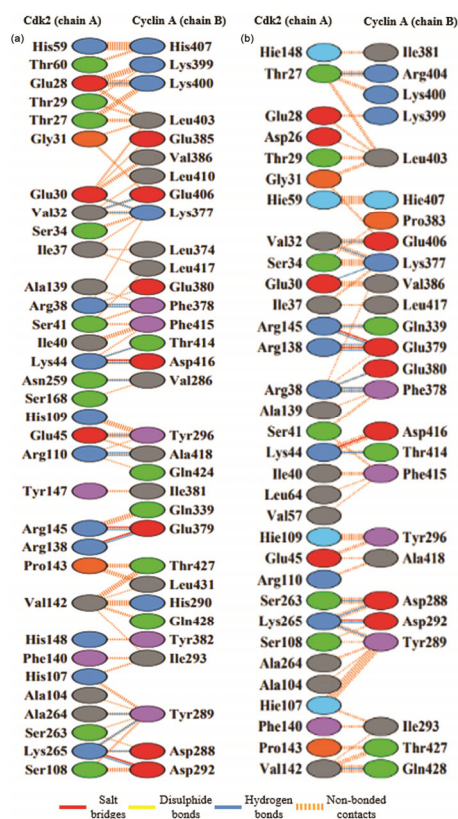


Fig. 9 — Interactive residues between chain A (Cdk2) and chain B (Cyclin A) (a) unphosphorylated system; and (b) phosphorylated system as predicted by PDBsum server. Molecular interactions such as hydrogen bonds, non-bonded contacts and salt bridges are considered here

Cdk2-cyclin A complex. The unphosphorylated interface involves 33 Cdk2 residues with interface area of 1721 Å² and 32 Cyclin A residues with an interface area of 1734 Å². There are 18 hydrogen bonds and 4 salt bridges (exclusive for Cdk2). Upon phosphorylation, the number of residues decreases to 32 in Cdk2 and significantly drops to 26 in Cyclin A. Corresponding reductions in interface area to 1644 Å² (Cdk2) and 1654 Å² (Cyclin A) was also observed. The number of hydrogen bonds falls to 17 while the number of salt bridges remains at 4. These changes indicate adjustments upon phosphorylation without eliminating

key interactions. The number of non-bonded contacts shows a significant reduction from 198 to 165 upon phosphorylation. This indicates a lower compactness and an overall loosening at the interface of the phosphorylated complex. Such structural changes could regulate enzymatic activity of the complex, regulation, or dynamic flexibility throughout cell cycle progression

Conclusion

Our study concludes that when the protein p27 is phosphorylated at Y74 and Y88 positions, there is an increase in the binding affinity of p27 to Cdk2/cyclinA complex. This may signify a larger interface area which makes it possible for more amino acid residues to interact among themselves, which strengthens the bonds. It is also found from the results of trajectory analyses such as SASA and RMSD that phosphorylated form of the complex shows greater stability. A drop in the RMSD values is observed which may show that the system is more stable and energy efficient after phosphorylation. Additionally, the stability of the complex is also enhanced due to the increase in the number of hydrogen bonds and non-bonded contacts. Although phosphorylation of p27 increases the interaction between Cdk2 and p27, there is a decrease in the interacting residue count and van der Waals interactions between Cdk2 and CyclinA, which weakens its association. Overall, our work highlights the role of phosphorylation of p27 in the regulation of cell cycle by controlling Cdk2 activity. This study may provide a foundation for future research in targeted therapies in cancer and other proliferative diseases.

Acknowledgement

The authors extend their deepest gratitude to Tezpur University and University Grants Commission, India, for the start-up grant and to Department of Molecular Biology and Biotechnology, Tezpur University for providing adequate computational facility.

Conflict of interest

All authors declare no conflict of interest.

References

- 1 Phillips AH & Kriwacki RW, The role of intrinsic protein disorder in regulation of cyclin-dependent kinases. *Curr Opin Struct Biol*, 88 (2024) 102906.
- 2 Russo AA, Jeffrey PD, Patten AK, Massagué J & Pavletich NP, Crystal structure of the p27Kip1 cyclin-dependent-kinase inhibitor bound to the cyclin A-Cdk2 complex. *Nature*, 382 (1996) 325.
- 3 Satyanarayana A & Kaldis P, Mammalian cell-cycle regulation: several Cdks, numerous cyclins and diverse compensatory mechanisms. *Oncogene*, 28 (2009) 2925.
- 4 Li Q, Jiang B, Guo J, Shao H, Del Priore IS, Chang Q, Kudo R, Li Z, Razavi P, Liu B, Boghossian AS, Rees MG, Ronan MM, Roth JA, Donovan KA, Palafox M, Reis-Filho JS, de Stanchina E, Fischer ES, Rosen N, Serra V, Koff A, Chodera JD, Gray NS & Chandarlapaty S, INK4 Tumor Suppressor Proteins Mediate Resistance to CDK4/6 Kinase Inhibitors. *Cancer Discov*, 12 (2022) 356.
- 5 Sherr CJ & Roberts JM, CDK inhibitors: positive and negative regulators of G1-phase progression. *Genes Dev*, 13 (1999) 1501.
- 6 Guiley KZ, Stevenson JW, Lou K, Barkovich KJ, Kumarasamy V, Wijeratne TU, Bunch KL, Tripathi S, Knudsen ES, Witkiewicz AK, Shokat KM & Rubin SM, p27 allosterically activates cyclin-dependent kinase 4 and antagonizes palbociclib inhibition. *Science*, 366 (2019) 2106.
- 7 Ou L, Waddell MB & Kriwacki RW, Mechanism of cell cycle entry mediated by the intrinsically disordered protein p27(Kip1). *ACS Chem Biol*, 7 (2012) 678.
- 8 Trivedi R & Nagarajaram HA, Intrinsically Disordered Proteins: An Overview. *Int J Mol Sci*, 23 (2022) 14050.
- 9 Uversky VN, Introduction to intrinsically disordered proteins (IDPs). *Chem Rev*, 114 (2014) 6557.
- 10 Iakoucheva LM, Brown CJ, Lawson JD, Obradović Z & Dunker AK, Intrinsic disorder in cell-signaling and cancer-associated proteins. *J Mol Biol*, 323 (2002) 573.
- 11 Yakubu UM & Morano KA, Suppression of aggregate and amyloid formation by a novel intrinsically disordered region in metazoan Hsp110 chaperones. *J Biol Chem*, 296 (2021) 100567.
- 12 Wright PE & Dyson HJ, Intrinsically disordered proteins in cellular signalling and regulation. *Nat Rev Mol Cell Biol*, 16 (2015) 18.
- 13 Zhu J, Salvatella X & Robustelli P, Small molecules targeting the disordered transactivation domain of the androgen receptor induce the formation of collapsed helical states. *Nat Commun*, 13 (2022) 6390.
- 14 Jarnot P, Ziemska-Legiecka J, Grynberg M & Gruca A, Insights from analyses of low complexity regions with canonical methods for protein sequence comparison. *Brief Bioinform*, 23 (2022) bbac299.
- 15 Davey NE, Shields DC & Edwards RJ, SLiMDisc: short, linear motif discovery, correcting for common evolutionary descent. *Nucleic Acids Res*, 34 (2006) 3546.
- 16 Lindorff-Larsen K, Piana S, Palmo K, Maragakis P, Klepeis JL, Dror RO & Shaw DE, Improved side-chain torsion potentials for the Amber ff99SB protein force field. *Proteins*, 78 (2010) 1950.
- 17 Jorgensen WL, Chandrasekhar J, Madura JD, Impey RW & Klein ML, Comparison of simple potential functions for simulating liquid water. *J ChemPhys*, 79 (1983) 926.
- 18 Homeyer N, Horn AHC, Lanig H & Sticht H, AMBER force-field parameters for phosphorylated amino acids in different protonation states: phosphoserine, phosphothreonine, phosphotyrosine, and phosphohistidine. *J Mol Model*, 12 (2006) 281.
- 19 Steinbrecher T, Latzer J & Case DA, Revised AMBER parameters for bioorganic phosphates. *J Chem Theory Comput*, 8 (2012) 4405.
- 20 Pines J, Cyclins and cyclin-dependent kinases: a biochemical view. *Biochem J*, 308 (1995) 697.
- 21 Berman HM, Battistuz T, Bhat TN, Bluhm WF, Bourne PE, Burkhardt K, Feng Z, Gilliland GL, Iype L, Jain S, Fagan P, Marvin J, Padilla D, Ravichandran V, Schneider B, Thanki N, Weissig H, Westbrook JD & Zardocki C, The protein data bank. *Acta Crystallogr D Biol Crystallogr*, 58 (2002) 899.
- 22 Case DA, Belfon K, Ben-Shalom IY, Brozell SR, Cerutti DS, Cheatham TE III, Cruzeiro VWD, Darden TA, Duke RE, Giambasu G, Gilson MK, Gohlke H, Goetz AW, Harris R, Izadi V, Izmailov SA, Kasavajhala K, Kovalenko A, Krasny R, Kurtzman T, Lee TS, LeGrand S, Li P, Lin C, Liu J, Luchko T, Luo R, Man V, Merz KM, Miao Y, Mikhailovskii O, Monard G, Nguyen H, Onufriev A, Pan F, Pantano S, Qi R, Roe DR, Roitberg A, Sagui C, Schott-Verdugo S, Shen J, Simmerling CL, Skrynnikov NR, Smith J, Swails J, Walker RC, Wang J, Wilson L, Wolf RM, Wu X, Xiong Y, Xue Y, York DM & Kollman PA, AMBER 2020. University of California, San Francisco (2020).
- 23 Pettersen EF, Goddard TD, Huang CC, Couch GS, Greenblatt DM, Meng EC & Ferrin TE, UCSF Chimera—a visualization system for exploratory research and analysis. *J Comput Chem*, 25 (2004) 1605.
- 24 Kräutler V, Van Gunsteren WF & Hünenberger PH, A fast SHAKE algorithm to solve distance constraint equations for small molecules in molecular dynamics simulations. *J Comput Chem*, 22 (2001) 501.
- 25 Berendsen HJC, Postma JPM, Van Gunsteren WF, DiNola A & Haak JR, Molecular dynamics with coupling to an external bath. *J Chem Phys*, 81 (1984) 3684.
- 26 Roe DR & Cheatham III TE, PTRAJ and CPPTRAJ: Software for Processing and Analysis of Molecular Dynamics Trajectory Data. *J Chem Theory Comput*, 9 (2013) 3084.
- 27 Tsytlonok M, Sanabria H, Wang Y, Felekyan S, Hemmen K, Phillips AH, Yun MK, Waddell MB, Park CG, Vaithiyalingam S, Iconaru L, White SW, Tompa P, Seidel CAM & Kriwacki R, Dynamic anticipation by Cdk2/Cyclin A-bound p27 mediates signal integration in cell cycle regulation. *Nat Commun*, 10 (2019) 1676.
- 28 Grimm M, Wang Y, Mund T, Cilenšek Z, Keidel EM, Waddell MB, Jäkel H, Kullmann M, Kriwacki RW & Hengst L, Cdk-inhibitory activity and stability of p27Kip1 are directly regulated by oncogenic tyrosine kinases. *Cell*, 128 (2007) 269.
- 29 Lobanov MY, Bogatyreva NS & Galzitskaya OV, Radius of gyration as an indicator of protein structure compactness. *Mol Biol*, 42 (2008) 623.
- 30 Durham E, Dorr B, Woetzel N, Staritzbichler R & Meiler J, Solvent accessible surface area approximations for rapid and accurate protein structure prediction. *J Mol Model*, 15 (2009) 1093.
- 31 Laskowski RA, Jabłońska J, Pravda L, Vařeková RS & Thornton JM, PDBsum: Structural summaries of PDB entries. *Protein Sci*, 27 (2018) 129.